Chain-Length-Dependent Termination Rate Processes in Free-Radical Polymerizations. 3. Styrene Polymerizations with and without Added Inert Diluent as an Experimental Test of Model

Peter A. G. M. Scheren,[†] Gregory T. Russell,[‡] David F. Sangster,[§] Robert G. Gilbert,[*,§] and Anton L. German[†]

Faculty of Chemical Engineering, Eindhoven University of Technology, 5600 MB Eindhoven, The Netherlands, Chemistry Department, University of Canterbury, Private Bag 4800, Christchurch, New Zealand, and School of Chemistry, Sydney University, Sydney, NSW 2006, Australia

Received September 28, 1994; Revised Manuscript Received February 10, 1995[⊗]

ABSTRACT: Experiments were performed to test a model for the kinetics of free-radical polymerization systems, including the dependence of the termination rate coefficients on the lengths of both chains involved. The model has few adjustable parameters, the values of which are moreover confined within fairly narrow limits. The data comprised the rate of polymerization in a seeded emulsion polymerization of styrene, with and without benzene as diluent, with initiation by persulfate and by γ-radiolysis. The latter can be switched off instantly, providing relaxation data which are sensitive to termination kinetics. Data from a single relaxation at a fixed weight-fraction polymer (w_p) were fitted to fix the unknown parameters, of which the only significant one is the probability p of reaction between two radicals upon encounter, incorporating the effect of spin multiplicity; this must lie between 0.25 and 1. Modeling using the value so obtained then successfully fitted (a) relaxation data at the same w_p but with 15 mol % benzene diluent, (b) relaxation data with and without diluent over the range $0.5 \leq w_p \leq 0.8$, and (c) chemically initiated data over the same w_p range. This provides convincing evidence for the correctness of the termination model, which calculates the termination rate coefficients between two chains from the Smoluchowski equation, incorporating p, with diffusion coefficients (as a function of chain length and of w_p) obtained from a "universal" scaling law inferred from NMR data, and where the interaction distance for termination is the van der Waals radius of a monomeric unit; contributions from "reaction diffusion" (whereby a chain end moves by propagating) are also important at high conversion. The data also support a model for initiator efficiency in emulsion polymerization, this model being based on competition between aqueous-phase propagation (to a sufficient degree of polymerization for surface activity) and termination.

1. Introduction

An understanding of termination kinetics is of fundamental importance in free-radical polymerization. This would serve to cast light on the mechanisms by which phenomena such as the Trommsdorff–Norrish or "gel" effect[1,2] occur. Moreover, an understanding of the subtleties of termination has been found indispensable in accurate prediction of molecular weight distributions.[3] Rate coefficients for termination between two carbon-centered radicals in liquids are usually high (unless the approach of the radical chain ends is hindered by bulky substituents[4,5]). Benson and North[6] pointed out that, since the chemical barrier for a reaction between two radicals is very low,[7] termination in a polymerizing system will usually be diffusion controlled. Because the diffusion of penetrants through a polymer matrix is slower for larger molecules, the termination rate coefficient for the propagating chains in such a system is likely to depend on the length of each radical chain,[6,8–17] as well as on the viscoelastic properties of the polymerizing medium.

The objective of the present paper is to carry out a test of a quantitative model for termination in free-radical polymerization systems. This model[16,17] provides for the dependence of the termination rate coefficients on the lengths of both chains involved and creates a means of predicting the kinetics and the molecular weight distributions[3] in any system with a minimum of adjustable parameters. Moreover, the values of the few parameters which need to be adjusted are confined within fairly narrow limits from independent experiments.

The system chosen for this test is that of a seeded emulsion polymerization, wherein the adjustable parameters are fixed absolutely from one measurement (the relaxation kinetics at a particular polymer weight fraction) and the results of quite different data (the kinetics of relaxation at different polymer fractions and with the addition of an inert diluent and the kinetics with chemical initiator over a wide range of polymer fraction) both can be measured experimentally and are precisely predictable from the model. This therefore provides a stringent test of the accuracy of the theory.

The kinetics measurements are performed on a seeded emulsion polymerization, in which monomer-swollen latex particles are the sole locus of polymerization and in which the number of these loci is predetermined as the number concentration of seed particles. Free-radical polymerization thus takes place in the presence of preformed polymer. A special means of deriving information for these kinetic studies is by performing γ-radiolysis emulsion polymerization experiments.[18–22] A feature of these experiments is that the γ-rays, the source of initiating radicals, can be cut off essentially instantaneously by removing the reactor from the ^{60}Co source. The kinetics are then dominated by radical-loss processes. If the size of the seed particles is chosen to

* Author to whom correspondence should be addressed.
† Eindhoven University of Technology.
‡ University of Canterbury.
§ Sydney University.
⊗ Abstract published in *Advance ACS Abstracts,* April 1, 1995.

0024-9297/95/2228-3637$09.00/0

be sufficiently large, then termination will be the sole radical-loss mechanism (as distinct from radical loss by exit, i.e., desorption, which is often the dominant loss mechanism for small particles but whose rate decreases with increasing particle size[23-27]). Kinetic data thus obtained from such *relaxation experiments* are sensitive to the model for termination events in the system. Moreover, these experimental systems, although formally heterogeneous, are bulklike in their kinetic behavior and are expected to display the same termination kinetics as would have been observed in equivalent bulk or solution systems.

Experimental data are reported here for seeded styrene emulsion polymerizations at intermediate to high weight fractions (w_p) of polymer, in the range of $0.5 \leq w_p \leq 0.95$. Experiments were also carried out where styrene seed latex was swollen with an inert diluent. The diluent used for this purpose was benzene, which because of its physical similarity to styrene is not expected to cause any significant changes in physical properties of the polymerizing system, while because of its chemical inertness in this particular system it should not compete in any radical reactions. For example, it has been shown (from the effect on the desorption rate coefficient[28] and from the benzene/styrene transfer constant[29]) that, in contradiction to other diluents such as ethylbenzene, toluene, and cyclohexane, radical transfer to benzene is kinetically insignificant in emulsion polymerizations. Moreover, no observable solvent effects of ethylbenzene on the styrene propagation rate coefficient (k_p) have been found,[30] suggesting that benzene also would not change k_p.

What effects might an inert diluent exert? Consider therefore two systems of identical w_p, one composed of just monomer and polymer, the other with the same fraction polymer but with the monomer concentration diluted by an "inert" diluent which does not affect properties such as viscosity and solvent power. A "classical" kinetic scheme predicts that the termination rate coefficient should be identical in both these systems. However, if termination were chain-length-dependent, then the diluent-containing system would have a higher overall termination rate coefficient. This is because in this system the monomer concentration is lower, and so radicals grow at a slower rate. This will result in the length distribution of growing radicals being more weighted toward smaller chain lengths. Because smaller radicals diffuse (and so terminate) faster than longer radicals, the rate of termination will be higher in the monomer-diluted system. So a change in the relaxation behavior with added inert diluent would support the concept of termination being chain length dependent. Further, quantitative modeling of the experimental data should provide a stringent test for any model for the dependence of the rate coefficients for termination on the lengths of the two radicals involved. A key point here is that, provided w_p is held constant, the "microscopic" termination rate coefficient k_t^{ij} (where i and j are the degrees of polymerization of the two chains) will not be changed by addition of diluent. However, because the diluted and undiluted systems will have different living radical chain length *distributions*, the *rates* of termination will nevertheless be different in these two otherwise identical systems. Also, by lowering the monomer concentration, an inert diluent will also lower the rates of other processes such as propagation, transfer, and (in emulsion polymerizations) exit.

Many workers[3,8-17] have presented microscopic descriptions of the termination processes in free-radical polymerizations, including the dependence of k_t^{ij} on i and j. Setting down kinetic equations for all individual free-radical species seems to result in an exceedingly complex process. However, Russell *et al.*[16,17] seem to be the first to have succeeded in reducing the full set of rate equations to a form which is easily solved numerically while at the same time avoiding making unphysical assumptions about the form of k_t^{ij} to facilitate the mathematics. Their model, which is adopted with minor changes in this paper, aims at a full physical description of all kinetic aspects of the processes involved. The kinetic runs in the present paper are designed to evaluate the ability of the model to predict different termination rate behavior under otherwise similar conditions and parameter choice.

2. Summary of Model

A concise summary of the model for termination kinetics[3,16,17] is now given, along with some minor extensions of the original treatment and the means by which accurate numerical solutions can be obtained.

It has long been realized that termination interactions in free-radical polymerizations are usually *diffusion controlled* (except perhaps for very small[31] or highly hindered[4,5] entities). In the classic work of Benson and North,[6] the idea of a three-step termination process was first established. They suggested that center-of-mass diffusion must first render two macroradicals proximate; the radical chain ends must next encounter each other (perhaps by "segmental" diffusion, by which is meant the diffusion consequent upon reorientational chain backbone motions of a macroradical); the final step is chemical reaction itself. As bimolecular termination involves reaction between two radicals, the energy barrier to reaction is small,[7] and therefore termination is usually diffusion controlled. Under such circumstances, the rate coefficient can be calculated by using the Smoluchowski expression

$$k_t^{ij} = 2\pi p_{ij} D_{ij} (r_i + r_j) N_A \qquad (1)$$

in which k_t^{ij} is the termination rate coefficient for termination between species of degrees of polymerization i and j, N_A is Avogadro's constant, $r_i + r_j$ is the radius of interaction (i.e., the reactant separation at which termination is supposed to occur instantaneously), D_{ij} is the mutual diffusion coefficient for diffusion of radical ends of chains of degrees of polymerization i and j, and the factor p_{ij} is the probability of reaction upon encounter, incorporating the effects both of spin multiplicity and of hindrance during solvent cage trapping (in the original treatment of Russell *et al.*[17] no account was taken of the possible dependence of p_{ij} on chain length). The different aspects involved in eq 1 will now be discussed.

Radius of Interaction. For reasons given in detail by Russell *et al.*,[16,17] a reasonable approximate treatment would seem to be to identify $r_i + r_j$ with σ, the Lennard-Jones diameter of a monomer unit, at least in systems above c^*.

Mutual Diffusion Coefficient. Because the long-time-scale diffusion of species i is unaffected by the long-time-scale diffusion of species j, the mutual diffusion coefficient D_{ij} can be partitioned into the sum of

contributions from each of the two radical species:

$$D_{ij} = D_i + D_j \tag{2}$$

D_i and D_j are the diffusion coefficients for each of the species i and j. For termination reactions, it is the motion of radical chain ends that is of interest. Since free radicals are, in general, widely separated, the rapid small-length-scale motions of the free-radical chain end can be ignored in specifying D_i, for these motions will not effectively bring two widely separated free-radical chain ends any closer (on the length scale of rapid, short-time-scale conformational motions). Two mechanisms contribute to the longer-length-scale motions: (1) center-of-mass diffusion of the chain as a whole, with diffusion coefficient D_i^{com}, and (2) diffusion by propagation of the chain end ("reaction diffusion"[32]), with a diffusion coefficient D^{rd} which is independent of chain length (at least for chains which are long and entangled, which are the only ones for which reaction diffusion is of kinetic significance[17]). Russell *et al.*[33] showed that

$$D^{rd} = \frac{1}{6} k_p C_M a^2 \tag{3}$$

Here C_M is the concentration of monomer in the locus of polymerization and a is the root-mean-square end-to-end distance per square root of the number of monomer units in a polymer chain (i.e., a is the mean distance moved, in a random flight sense, at each propagation step). Hence, one has:

$$D_i = D_i^{com} + D^{rd} \tag{4}$$

The dependence of D_i upon the degree of polymerization i and on w_p can be conveniently written in the form of a general scaling law:

$$D_i^{com}(w_p) = \frac{D_{mon}(w_p)}{i^{u}(w_p)} \tag{5}$$

In eq 5, $D_{mon}(w_p) \equiv D_1^{com}(w_p)$ is the diffusion coefficient of monomer at a given w_p, and $u(w_p)$ is an exponent, which may depend on conversion (w_p), specifying how the diffusion coefficient varies with i. Equation 5 will be considered in more detail later in this paper.

Spin Multiplicity and Hindrance. If p_{ij} were 1, eq 1 would state that every encounter of radical chain ends results in termination. However, this is first complicated by the effect of spin multiplicity.[7,17,34,35] Each radical (being a doublet) can be in one of two possible spin states. Termination by combination can only occur if two encountering radicals have opposite spins, in which case they recombine along the singlet-state electronic surface. The probability for this is $^1/_4$ (since two randomly chosen radicals might have the same spin, in which case they are on a triply degenerate triplet surface). Hence, for cases where the characteristic time scale for spin flipping is much longer than the typical time scale of radical encounter, p_{ij} would take the value $^1/_4$. Now, for the encounter of two polymer chain ends, the latter time scale is determined by the duration of solvent cage trapping. For very short, unentangled chains in solution, the rate of encounter is expected to exceed that of spin flipping,[34,35] and for those cases p_{ij} in eq 1 would therefore be expected to be close to $^1/_4$. However, the typical duration of a solvent cage trapping event may be caused to be much longer under two types of circumstances: if either the radicals are long and entangled or the system has a high microviscosity. Hence, for a polymerization reaction at intermediate to high w_p, p_{ij} should be unity for recombination reactions involving two long chains. Thus p_{ij}, incorporating the effect of spin multiplicity, should be a function of chain length and of w_p.

In addition to the effect of spin multiplicity, the termination rate coefficient can be reduced below the Smoluchowski value if close-range radical encounter is highly hindered (e.g., refs 4 and 5) (and in such cases, termination might occur by disporportionation instead of combination[34]). If the terminating species encounter each other in such a way that once in a solvent cage they cannot reorient to overcome steric hindrance, the factor p_{ij} can be used to modify the Smoluchowski result and might then be even lower than $^1/_4$, the minimum value given for the effect of spin multiplicity above.

Kinetic Equations. The second aspect of model development is to set down rate equations suitable for incorporation of chain-length-dependent termination. In this section we give a minimal summary of the treatment of Russell *et al.*[16,17] The starting point is to note that emulsion polymerization systems such as the present wherein termination is rate-determining usually have a high value of $\bar{n}$, the average number of radicals per latex particle. Under those circumstances, the kinetics can be expressed in terms of the "pseudobulk" approximation, where the effect of free radicals being compartmentalized into latex particles may be ignored. In other words, each particle may be considered to be bulk polymerization-like in its kinetic behavior. Denote by R_i the population of radicals of degree of polymerization i in a particular particle; these R_i are normalized so that:

$$\sum_{i=1}^{\infty} R_i = \bar{n} \tag{6}$$

The time evolution of R_i is found by taking account of radical entry into a particle (which is assumed to occur at some degree of polymerization z, as discussed elsewhere[26,36]), transfer, termination, and propagation. Because the present system involves large particles, radical loss by exit (desorption) into the aqueous phase is negligible[27] and so can be ignored. The required population evolution equations are then:

$$\frac{dR_1}{dt} = \varrho\delta_{1z} + k_{tr}C_M\sum_{i=2}^{\infty}R_i - k_p{}^1C_MR_1 - 2R_1\sum_{i=1}^{\infty}c^{1i}R_i \tag{7}$$

$$\frac{dR_i}{dt} = \varrho\delta_{iz} + (k_p{}^{i-1}R_{i-1} - k_p{}^iR_i)C_M - k_{tr}C_MR_i - 2R_i\sum_{j=1}^{\infty}c^{ij}R_j, \quad i \geq 2 \tag{8}$$

Here $k_p{}^i$ is the propagation rate coefficient of an i-meric radical, ϱ is the pseudo-first-order rate coefficient for entry, k_{tr} is the rate coefficient for transfer, and c^{ij} is the pseudo-first-order rate coefficient for termination between an i- and a j-meric radical. This last is related

to the usual second-order termination rate coefficient by:

$$c^{ij} = k_t^{ij}/N_A V_s \tag{9}$$

where V_s is the swollen volume of a latex particle (the latex is taken to be monodisperse in size, which is readily achieved experimentally with a seeded emulsion polymerization). The entry rate coefficient in a system such as the present in which radical exit, and hence reentry, can be ignored is the sum of components from radicals arising directly from initiator and from "thermal entry".[37-39] The latter is a relatively small source of radicals which possibly arises from reactions of adventitious species on the surface of the particles. One thus has

$$\varrho = \varrho_{\text{initiator}} + \varrho_{\text{thermal}} \tag{10}$$

Note that here all free-radical concentrations have been assumed to be spatially homogeneous, eliminating the possibility of radical concentration gradients in the latex particles. It is, however, conceivable that even in emulsion homopolymerizations a gradient occurs due to hydrophilic end groups of initiator-derived entering species being fixed at the surface ("surface anchoring"), this acting together with diffusion being relatively slow. However, extensive modeling and experiment[40-42] show that no inhomogeneities are likely for styrene emulsion polymerizations of the particle size and monomer concentration range employed here.

The next step is to obtain means for solving eqs 7 and 8 numerically. Extensive simulation[16,43] has shown that, for intermediate and high conversion conditions, a solution of quite acceptable accuracy for modeling conversion (but *not* molecular weight distributions[3]) can be obtained as follows. First, the steady-state approximation is made for some of these equations (see below). Next, one makes the "short-long" approximation: assuming that the rate at which a short chain terminates depends only on the rate at which the short chain diffuses and not on that of the chain with which it is terminating. The basic reason for the accuracy of this approximation is that most termination events involve a relatively short, mobile chain and a longer entangled one, because long chains form an overwhelming majority of radical species present in the system. A rapidly diffusing short radical chain will thus have a higher probability of terminating by encountering a long radical chain than by encountering another short radical chain. The next approximation is to consider radicals of chain length exceeding a certain critical degree of polymerization, Z, as being kinetically identical. One may wish to think of Z as a physical parameter, marking the degree of polymerization at which chains become "long" and entangled. However, Z is no more than a numerical parameter, which must be made sufficiently large that the solutions of the above equations become independent of its value. The values of the R_i for $i \leq Z$ can be found from the approximate relationship deduced from the steady-state treatment of eqs 7 and 8:

$$R_1 = \frac{\varrho\delta_{1z} + k_{tr}C_M\bar{n}}{k_p{}^1C_M + 2c^{1L}\bar{n}} \tag{11}$$

$$R_i = \frac{\varrho\delta_{iz} + k_p{}^{i-1}C_M R_{i-1}}{k_p{}^iC_M + k_{tr}C_M + 2c^{iL}\bar{n}}, \quad 2 \leq i \leq Z \tag{12}$$

Here c^{iL} is the value of c^{ij} for termination between an i-mer and any long chain; since, for small i, $D_i^{com} \gg D_L^{com}$, a long chain may be taken as having a zero value for its center-of-mass diffusion coefficient (see eq 4). The total population of all radicals of degree of polymerization greater than Z is denoted P, for which one has the relations:

$$\bar{n} = \sum_{i=1}^{Z} R_i + P \tag{13}$$

$$\frac{dP}{dt} = k_pC_MR_Z - k_{tr}C_MP - 2c^{LL}P^2 - 2P\sum_{i=1}^{Z} c^{iL}R_i \tag{14}$$

Equations 11–14 are solved numerically. An appropriate value of Z is determined by carrying out kinetic simulations covering an appropriate range of conditions applicable to the experiment and increasing Z until the calculated time dependence of $\bar{n}$ becomes Z-independent.[16] For the present system, it was found that $Z \geq 180$ was adequate, and so $Z = 180$ was used in the simulations carried out here. Once a value of Z has been established, a quicker numerical solution can be found, noting that, providing Z is not too large, $\bar{n} \approx P$. Hence, one may put $\bar{n} = P$ and replace eqs 13 and 14 with

$$\frac{d\bar{n}}{dt} = k_pC_MR_Z - k_{tr}C_M\bar{n} - 2c^{LL}\bar{n}^2 - 2\bar{n}\sum_{i=1}^{Z} c^{iL}R_i \tag{15}$$

There are no significant differences between the solutions so obtained and those of numerically exact solutions[16] (which require the full solution of the nonlinear, coupled eqs 7 and 8).

Experimental data comprise fraction conversion x as a function of time. This can be converted to an experimental value of $\bar{n}$, or the calculated $\bar{n}$ (found by solution of eqs 15, 11, and 12) converted to a calculated $x(t)$, using the relation

$$\frac{dx}{dt} = \frac{k_pC_M\bar{n}N_c}{n_M{}^0N_A} \tag{16}$$

Here N_c is the number of latex particles per unit volume of the aqueous phase, and $n_M{}^0$ is the initial number of moles of monomer present per unit volume of the aqueous phase.

The complete solution of the evolution equations is thus to solve eqs 15 and 16 numerically; in order to evaluate eq 15, values of R_i are obtained from using eqs 11 and 12, with the value of $\bar{n}$ from calling the differential equation solver being used. This treatment allows solutions to be computed easily, quickly, and accurately and can be used for routine fitting of experimental rate data.

It is important to note that the fully microscopic description of termination kinetics given here, in either the complete form of eqs 7 and 8 or the approximate form of eq 15, can only be written in a conventional form, $d\bar{n}/dt = \varrho - 2k_t\bar{n}^2/N_AV_s$, if the termination rate coefficient therein is actually an *average* over chain lengths. Formally, by summing over eqs 7 and 8 (for all i) one can always write:

$$d\bar{n}/dt = \varrho - 2\langle k_t\rangle\bar{n}^2/N_AV_s \tag{17}$$

Table 1. Details of Kinetics Runs

	PS2	PSR2	PSR5
initiating source	$K_2S_2O_8$	γ-ray	γ-ray
[initiator]/dose rate	11.21×10^{-4} mol dm^{-3}	95.3 Gy h^{-1}	95.3 Gy h^{-1}
initial conditions			
diluent mole fraction	0	0	0.15
starting w_p	0.495	0.498	0.500
C_M/(mol dm^{-3})	4.62	4.60	3.89
N_c/dm^{-3}	3.6×10^{15}	3.7×10^{15}	3.6×10^{15}

Table 2. Concentrations of Styrene in the Aqueous Phase as a Function of the Ratio d_f, the Fraction (moles of benzene)/(moles of benzene + moles of styrene) Added to the Unswollen Latex

	0.0	0.15	0.50	1.0
[styrene]/(mol dm^{-3})	4.66×10^{-3}	2.28×10^{-3}	1.93×10^{-3}	
[benzene]/(mol dm^{-3})		2.73×10^{-3}	6.44×10^{-3}	11.4×10^{-3}

but the termination rate coefficient therein is actually an average over all chain lengths (e.g., ref 16):

$$\langle k_t \rangle = \frac{\sum_i \sum_j k_t^{ij} R_i R_j}{(\sum_i R_i)^2} \tag{18}$$

That is, eqs 17 and 18 cannot be solved without knowing the time evolution of the R_i, which in turn can only be found by solving the more complete equations. However, defining an average or overall termination rate coefficient $\langle k_t \rangle$ can be useful, as will be seen.

3. Experimental Details

In order to ensure that the kinetics were pseudobulk and that radical loss by exit could be ignored, a large-size seed latex was employed. This was made using the recipe of Adams *et al.*:[20] 450 g of H_2O, 0.95 g of $NaHCO_3$ (buffer), 3.50 g of Aerosol MA 80 (sodium dihexylsulfosuccinate) as surfactant, 200 g of distilled styrene, and 0.86 g of $K_2S_2O_8$ (initiator), this being left to polymerize for 20 h at 50 °C. The resulting latex was filtered to remove any coagulum and dialyzed in order to remove excess surfactant, initiator, and buffer. The number-average particle size was 185 ± 4 nm (determined by transmission electron microscopy), with a solids content of 26.12%.

Seeded styrene interval III emulsion polymerizations were carried out in a dilatometer fitted with an automated tracking device that measured the contraction of reaction volume as a result of the conversion of monomer into polymer, and hence conversion as a function of time. Experiments were done both with pure (distilled) styrene as monomer and with styrene diluted with 15 mol % benzene (relative to the total number of moles of styrene and benzene) as inert diluent. Some kinetic runs were performed using a chemical initiator, $K_2S_2O_8$; others employed ^{60}Co γ-radiation as the initiating source; the temperature was maintained at 50 °C. The use of γ-initiation permits relaxation experiments: the polymerization vessel could be placed into and removed from the source with a lag of time of approximately 7 s. Removal from the source in this way results in nearly instantaneous switching off of any initiation (except for thermal generation of primary free radicals), and thus the decrease in observed polymerization rate is sensitive to radical loss mechanisms. Details of the experimental setup have been given elsewhere.[19] Several relaxations were made in each γ-initiated run. Experimental details of the kinetic runs are given in Table 1.

A knowledge of the partitioning of monomer between polymer particles and the aqueous phase will emerge as being required for modeling the entry process. It is expected that the concentration of styrene in the aqueous phase will be lowered in the presence of benzene. This partitioning was examined by swelling the seed latex with benzene/styrene at different ratios, with the total amount of solvent always corresponding to $w_p = 0.75$, an average w_p for our kinetic runs (see Table 1). The latex was allowed to swell for 18 h, while vigorously shaking. The samples were next ultracentrifuged for 1 h at 5×10^4 rpm and 20 °C to separate the aqueous phase. Concentrations of styrene and benzene in the aqueous phase were determined by GC, using isopropyl alcohol as an internal standard. The results of the monomer partitioning experiments are shown in Table 2.

Literature values for aqueous-phase solubilities at 50 °C for 100% styrene and 100% benzene are 4.3×10^{-3} [44] and 10.5×10^{-3} mol dm^{-3}, respectively. Table 2 shows that the difference between the solubilities at 20 and 50 °C is small enough to draw some conclusions about partitioning at 50 °C (where our polymerizations were performed) from the partitioning data at 20 °C (for technical reasons it was not possible to separate the serum phase at 50 °C). Table 2 shows that the aqueous phase concentration of styrene is reduced by about 50% when replaced by 15 mol % benzene but decreases only slowly as the mol percent benzene is further increased. Kinetic events controlled by the styrene aqueous-phase concentration are therefore likely to be influenced significantly by using benzene to dilute the monomer in an emulsion polymerization system. There is strong evidence[26,32] that entry of radicals arising from a chemical initiator is indeed influenced by aqueous-phase monomer concentration, and hence a significant effect on initiator efficiency is predicted for the system when benzene is added as an inert diluent.

4. Model Parameters

The overall strategy for testing of the termination model described above is to establish firm values of as many parameters as possible, to fix the remaining from fitting as little of the present data as possible, and then to see if the resulting parameters can fit the remaining data. The data fitting will be on the time evolution of both conversion and $\bar{n}$ (equivalent to the rate of polymerization). Although $x(t)$ and $\bar{n}(t)$ are trivially related through eq 16, comparison between model and experiment through these different observables provides different sensitivity to the model assumptions. In particular, a small difference in $\bar{n}$ between theory and experiment in a w_p range where $\bar{n}$ is changing rapidly can lead to a large difference in conversion at a later time (as illustrated later in this paper). For that reason, the most informative way to compare model and experiment in systems where termination plays a dominant kinetic role is through the dependence of $\bar{n}$ (i.e., radical concentration) on w_p.

Styrene emulsion polymerization systems are well characterized and have been much used for mechanistic studies. Consequently, many parameters required for the model are available within reasonable error limits. However, values of some parameters are still subject to significant uncertainty: (i) the value of k_p for short chains (as opposed to the long-chain value, which is accurately known[19,45-47]) (as required in eqs 11 and 12); (ii) the factor p_{ij}, representing the effects of spin

multiplicity and hindrance in radical termination reactions (required in eq 1); (iii) the thermal component of entry (see eq 10); (iv) the exact dependence of the diffusion coefficients of monomeric species on polymer weight fraction (eq 5); (v) the scaling laws for diffusional behavior of chains of different degrees of polymerization (also in eq 5); and (vi) the radius of interaction for termination (eq 1). For most of the above parameters, it will be seen that either values could be estimated from the literature with some degree of confidence, or the rate data are insensitive to the choice of these parameters, or a value can be determined precisely from part of the present data. Eventually really only the spin multiplicity/hindrance factor p_{ij} is left as adjustable in the present fitting; for the present conditions, no independent experimental information on this quantity is yet available.

We now consider all of the rate coefficients required for modeling the data.

Entry. The rate of entry of radicals into latex particles, as well as the character of these entering species, depends on the initiating source used. In an emulsion polymerization, radical generation occurs from chemical (or radiolytic) initiator and background thermal entry, as in eq 10. The model of Maxwell *et al.*[26,36] has been shown to reproduce a wide range of data on ϱ (or equivalently, the initiator efficiency) in emulsion polymerizations with persulfate as initiator. This model assumes that entry occurs only when an oligomeric radical formed by aqueous-phase propagation of the initiator decomposition product attains a certain critical degree of polymerization z in the aqueous phase. The rate-determining steps in this mechanism are thus propagation and termination of radicals in the aqueous phase, rather than the much faster diffusion of radicals to the latex particles. In summary, these reactions are:

$$\text{initiator} \xrightarrow{k_d} 2\text{I}^\bullet \tag{19}$$

$$\text{I}^\bullet + \text{M} \xrightarrow{k_{pi}} \text{IM}^\bullet \tag{20}$$

$$\text{IM}_n^\bullet + \text{M} \xrightarrow{k_{p,aq}{}^n} \text{IM}_{n+1} \tag{21}$$

$$\text{IM}_n^\bullet + \text{T}^\bullet \xrightarrow{k_{t,aq}} \text{inert products}, \quad n < z \tag{22}$$

$$\text{IM}_z^\bullet + \text{latex particle} \rightarrow \text{entry} \tag{23}$$

where T$^\bullet$ is any aqueous-phase free radical. The reactions of eqs 20 and 23 are supposed to be so fast as not to be rate-determining. If the aqueous-phase propagation and termination rate coefficients are assumed to be independent of degree of polymerization, the final result of this model then is

$$\varrho_{\text{initiator}} = \frac{2k_d[\text{I}]N_A}{N_c}\left\{\frac{(k_d[\text{I}]k_{t,aq})^{1/2}}{k_{p,aq}C_W} + 1\right\}^{1-z} \tag{24}$$

where C_W is the concentration of monomer in the water phase. The corresponding expression for the initiator efficiency f (i.e., comparing with the value of $\varrho_{\text{initiator}}$ assuming no aqueous-phase termination) is:

$$f = \left\{\frac{(k_d[\text{I}]k_{t,aq})^{1/2}}{k_{p,aq}C_W} + 1\right\}^{1-z} \tag{25}$$

Allowance for chain-length dependence can be made if so desired.[26] The value of $k_{p,aq}$ in the present treatment is assumed to be the same as for a long polymer chain (2.6×10^2 dm^3 mol^{-1} s^{-1} at 50 °C for styrene[37,46,47]), while the other values are $k_{t,aq} = 3.7 \times 10^9$ dm^3 mol^{-1} s^{-1},[48-50] $k_d = 8 \times 10^{-7}$ s^{-1},[36,51,52] and z between 2 and 3.[26,36] The large value for $k_{t,aq}$ being some 2 orders of magnitude faster than the termination of two *macro*radicals at low conversion, can be understood by noting that the latter $\langle k_t \rangle$ are averages over a very wide range of chain lengths, whereas the value of $k_{t,aq}$ is for tiny oligomers, and these will terminate by very rapid center-of-mass diffusion.[36] The saturated value of C_W was taken as 4.3×10^{-3} mol dm^{-3},[44] and this was scaled as[36,53] $C_W/C_W^{sat} = (C_M/C_M^{sat})^{0.6}$, where the superscript "sat" refers to the fully saturated value). The effect of dilution with benzene was taken into account by scaling C_W according to the data of Table 2.

During a γ-relaxation experiment, all external initiation sources are absent and only the thermal component, ϱ_{thermal}, remains. As the characteristics of this type of radical generation and entry are not yet understood, the thermal entry rate coefficient has to be taken as an adjustable parameter in our model. However, this quantity has virtually no effect on the initial shape of relaxations, which is completely dominated by termination (as is apparent from the fact that the final value of $\bar{n}$ after relaxation is typically an order of magnitude smaller than that at the instant of removal from the source, indicating that ϱ_{thermal} is very small). The value of ϱ_{thermal} only influences the (small) long-time value of $\bar{n}$ in a relaxation run and therefore is unimportant with regard to our major aim of understanding termination kinetics.

Propagation. Propagation can become diffusion-controlled at high conversion, and hence may depend on w_p. To avoid this complication, all relaxation data in this paper were obtained at w_p lower than that at which the monomeric diffusion coefficient starts to drop very rapidly. Hence, it can be assumed that k_p is independent of w_p in our relaxation experiments. The value for this quantity is that cited above, $k_p = 2.6 \times 10^2$ dm^3 mol^{-1} s^{-1}.

Because short radicals (formed only by transfer, in a relaxation experiment) are very mobile, they are important in overall termination kinetics; hence, it is necessary to have an accurate physical picture of the population of the shortest species, and hence how rapidly these propagate. It is likely (on the basis of both simple steric arguments[54] and indirect experimental evidence[27]) that the value of k_p for monomeric radicals, and even for somewhat longer species, could well be significantly greater than the long-chain k_p value. Recent data[27] suggest that for styrene polymerizations at 50 °C k_p^1 is approximately 4 times the long-chain value. Because we expect larger values for other short chains as well, in our simulations we put $k_p^1 = 4k_p$, $k_p^2 = 3k_p$, and $k_p^3 = 2k_p$. For $i > 3$ we use $k_p^i = k_p$.

Transfer. The transfer rate coefficient k_{tr} will not depend on w_p, provided that k_p is also independent of w_p.[55] The value used here[20] is 9×10^{-3} dm^3 mol^{-1} s^{-1}; however, there is a fairly wide range of values for this quantity in the literature.[29] Because transfer of radical

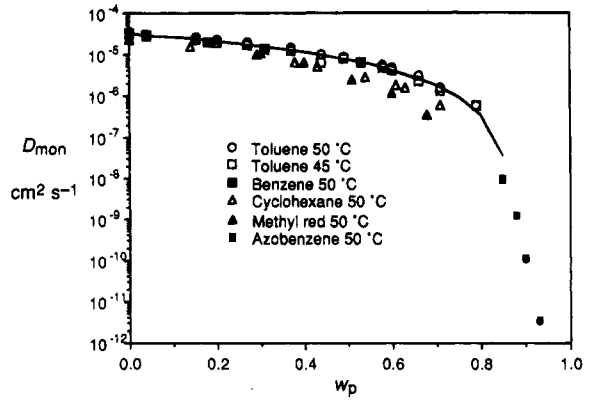

Figure 1. Diffusion coefficients for styrene-analog penetrants in polystyrene at various w_p and the indicated temperatures. Sources: toluene from ref 57; benzene from ref 58; cyclohexane from refs 58 and 59; methyl red from ref 60; azobenzene from refs 61 and 62. Line: polynomial fit of eq 26.

activity from entangled long-chain radicals to rapidly moving short-chain radicals has a profound influence on termination kinetics, the sensitivity to the choice of this parameter must be taken into consideration in our model evaluation.

Termination. It remains to define all parameters determining the termination rate coefficients. The values of σ and a were 0.60 and 0.74 nm, respectively.[16,56] The diffusion coefficient of monomer, D_{mon} (eq 5), at a given w_p was taken to be given by:

$$D_{mon}/(cm^2\ s^{-1}) = 3.188 \times 10^{-5} - 5.607 \times 10^{-5} w_p + 4.078 \times 10^{-6} w_p^{\ 2} + 2.096 \times 10^{-5} w_p^{\ 3} \quad (26)$$

This relation was obtained by fitting data for diffusion coefficients of styrene-analog penetrants[57-62] in solvent/polystyrene systems over the w_p range 0.0−0.8 (Figure 1). However, diffusion coefficients for styrene itself have not been measured as a function of w_p, and as well it is noticeable that small-molecule D values from different sources differ by up to a factor of 2. Hence, there is some flexibility in the value of D_{mon}. However, varying this quantity slightly is numerically (although certainly not physically) equivalent to varying p_{ij} through eq 1. The same also applies for uncertainty in σ. For this reason and as discussed later, we shall choose to treat p_{ij} as a single adjustable parameter that also incorporates uncertainty in D_{mon} and σ.

The dependence of the scaling parameter of eq 5, $u(w_p)$, on the degree of polymerization i was taken to be that found to fit a range of data for the diffusion of oligomers in polystyrene:[63,64]

$$u(w_p) = \min(2, -^1/_2 - 1.75 w_p) \quad (27)$$

This dependence goes smoothly from the dilute solution exponent of $^1/_2$ to the reptation value of 2 at high w_p. Since the data from which eq 5 was obtained were for oligomeric species whose degree of polymerization did not exceed 5, it is also necessary to consider how longer chains diffuse. Given the high polymer concentrations of the intermediate and high conversion conditions that prevailed in our experiments, it is reasonable to use a reptation power law ($D_i^{com} \sim i^{-2}$) for diffusion of long chains. It then only remains to specify how $u(w_p)$ varies with i. A semiempirical approach[16,17] here is simply to define a critical chain length X_c at which $u(w_p)$ changes from its small-chain value (eq 27) to its long-chain value of 2. Putting all this together and paying attention to the need for D_i^{com} to be continuous at $i = X_c$, one has:

$$D_i^{com}(w_p) = \begin{cases} \dfrac{D_{mon}(w_p)}{i^{u(w_p)}}, & i < X_c \\ \dfrac{D_{mon}(w_p) X_c^{\,2-u(w_p)}}{i^2}, & i \geq X_c \end{cases} \quad (28)$$

In the above equation, $u(w_p)$ is given by eq 27 and X_c is related[16,17] to the volume fraction of polymer, ϕ_p, by

$$X_c = X_c^{\,0}/\phi_p \quad (29)$$

It remains to specify a value for X_c^0. Simulations showed that the data are insensitive to this value provided it exceeds about 4; X_c^0 was therefore fixed as 4.

Spin/Hindrance Factor. The factor p_{ij} might in principle take any value in the range $0 \leq p_{ij} \leq 1$. However, if (as is the case with styrene) radical encounter is not sterically hindered, one expects $p_{ij} \geq {}^1/_4$. It is further necessary to ascertain how this quantity depends on the degrees of polymerization i and j of the two terminating chains. If both chains are sufficiently long to be relatively immobile, then it is likely that, in the event of diffusive encounter, the radical ends will be trapped in close proximity for sufficiently long for spin flips always to occur, in which case $p_{LL} = 1$. We shall henceforth assume, somewhat arbitrarily, that $p_{ij} = 1$ if both i and j exceed 10 and that otherwise all p_{ij} take the same value, which we denote p. The value of this quantity will be fixed by fitting one set of relaxation data and then subjected both to testing against other data and to a sensitivity analysis. This illustrates that data fitting cannot yield an *absolutely unique* set of parameters (i.e., values of all the p_{ij}). However, different parameter sets which fit the data were all found to give effectively the same population distribution R_i.

Initial Data Fitting. The parameters which may be varied are therefore p and $\varrho_{thermal}$. We now turn to actual data fitting. The strategy is first to fit the unknown parameters to one set of data. Figure 2 compares data obtained under relaxation conditions at $w_p = 0.71$ from an experimental system (run PSR2) which contained no diluent. The value of $\bar{n}$ at the time of removal from the radiation source was $\bar{n} = 29.7$. The data are compared to simulations with parameters chosen as above, with both p and $\varrho_{thermal}$ varied. The comparisons are made with both conversion and $\bar{n}$. In all simulations of relaxations, the initial value of $\bar{n}$ is set to that observed experimentally. Later when comparisons are made with chemically initiated data, the value of $\bar{n}$ will be set initially to an observed value and thereafter allowed to evolve; this approach tests the ability of the model to predict the gel effect (regime of rate acceleration) properly.

Referring to Figure 2, the first point of note is that, as seen from the experimental and model variations of $\bar{n}$ with time, the fully physical microscopic description of termination events in the system is in basic accord with experimental kinetic data: even without any fine tuning of adjustable parameters, reasonable agreement between experimental and simulated kinetics is obtained.

As shown in Figure 2, excellent accord between model and experiment can be obtained by assigning $p = 0.35$ and $\varrho_{thermal} = 0.027\ s^{-1}$. (Note that the value $z = 1$ was used for all fitting of relaxation data.) Recall here that

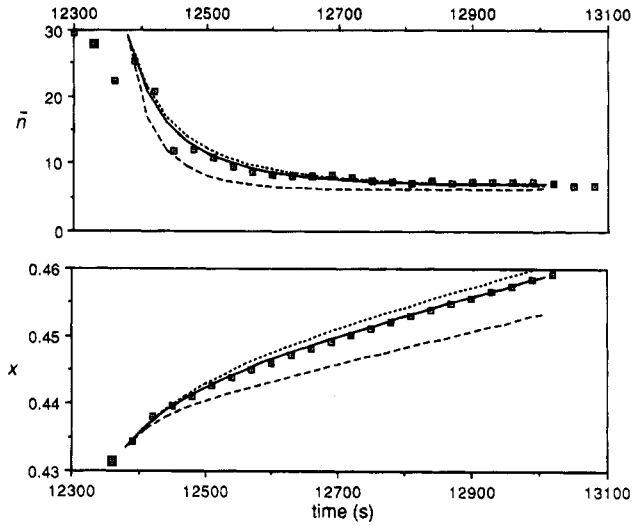

Figure 2. Fraction conversion x and $\bar{n}$ as functions of time after removal from the radiation source (relaxation data) for a system without benzene diluent (run PSR2). Time measured from start of run; removal from source occurred at 12 300 s. Initial: $w_p = 0.71$. Points: experiment. Lines: simulations; (···) $p = 0.25$, $\varrho_{thermal} = 0.022$ s^{-1}; (- - -) $p = 1$, $\varrho_{thermal} = 0.05$ s^{-1}; (—) $p = 0.35$, $\varrho_{thermal} = 0.027$ s^{-1}. The scatter in early-time experimental $\bar{n}$ in this and other plots is the result of numerical differentiation of noisy data when the system is changed very rapidly by removal from the radiation source.

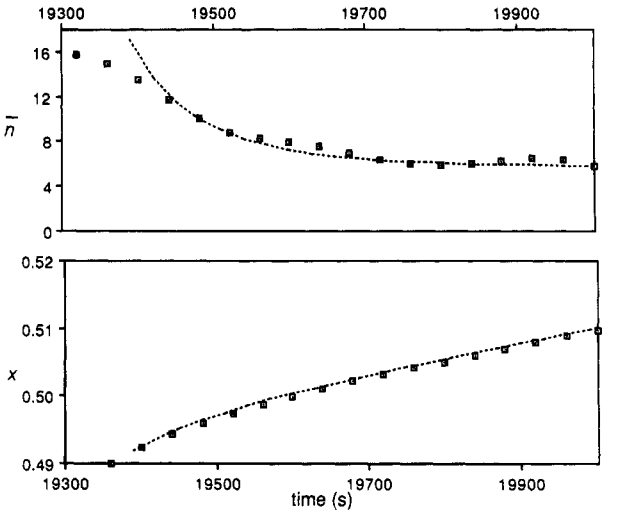

Figure 3. Fraction conversion x and $\bar{n}$ as functions of time after removal from the radiation source (relaxation data) with 15 mol % benzene as diluent. Time measured from start of run; removal from source occurred at 19 300 s. Initial $w_p = 0.71$. Points: experiment. Lines: simulation with same parameters as give best accord with experimental data in Figure 2.

in calculating k_t^{iL}, where $i \leq 10$ (see above), this adjustment of p is numerically equivalent to a slight adjustment in the assumed values of either D_{mon} (eq 26) or the interaction distance σ (used in eq 1). Some results of sensitivity analyses of our chosen parameters are given in Figure 2 in order to show the effect of parameter change in fitting thermal relaxation data. Provided its value is always chosen to give accord with the long-time value of $\bar{n}$ (i.e., that well after removal from the source), the value of $\varrho_{thermal}$ has no significant effect on the overall relaxation behavior, as illustrated in Figure 2.

Equally good accord between model and experiment can be obtained by minor adjustments of some other parameters within acceptable uncertainties. Although the (long-chain) value of k_p for styrene is now accurately known,[19,45-47] the values of k_p^i for smaller chains are not. Variation of k_p^i has a large effect on the simulated relaxation rate, for reasons outlined above: small chains are the most mobile and hence terminate most rapidly, and if (say) k_p^1 is large, then the most mobile chains will more quickly grow into less mobile ones, and so cause less termination. Hence, changing k_p^i significantly changes the simulated kinetics and the population distribution of the R_i. The effect on our simulations of changing k_p^i is indistinguishable from that of changing p, i.e., variation of either k_p^i or p can be used for data-fitting optimization.[17] Similar conclusions also hold for variation of k_{tr} within the uncertainties in the literature data.

Another aspect of our data fitting concerns the behavior observed over the very initial portions of our γ-relaxations. Referring to Figure 2 and subsequent figures showing relaxation data, it is evident that a slight time lag between removal from the γ-source and commencement of relaxation kinetics proper was always observed. Only a portion of this delay can be explained by the time necessary (approximately 7 s) for actual removal of the reaction vessel from the γ-source region. We therefore tentatively suggest that the cessation of entry of γ-derived radicals is not "instantaneous" upon removal from the γ-source. A possible scenario here is that, although these entering radicals are quickly adsorbed onto a particle surface,[36] their absorption into the monomer-rich particle interior is hindered and so is relatively slow: on the order of 1 min. No termination model can explain this time-lag phenomenon, for no termination model can give $-d\bar{n}/dt$ being greater at lower $\bar{n}$ than at higher $\bar{n}$. As shown in the figures, in our modeling we have side-stepped this intriguing problem simply by commencing simulations at a t and $x(t)$ that actually corresponded to a little while after removal from the γ-source.

5. Model Predictions

The correctness of the physical description of termination kinetics given here, and of the minor parameter adjustments discussed in the preceding section, can now be put to the test by seeing if data obtained with quite different populations of chain lengths can be reproduced. Since $p = 0.35$ and $\varrho_{thermal} = 0.027$ s^{-1} gave optimal agreement between model and experiment in Figure 2, we adopt these as "benchmark" values for attempting *a priori* reproduction of different experimental data in the following section of work.

Simulations of Relaxation Kinetics with Diluent. Diluting monomer in the latex particles with 15% of a chemically and physically inert diluent, benzene, has a large effect on the observed relaxation kinetics, as seen by comparing the experimental points shown in Figures 2 and 3: these are for undiluted and diluted systems with the same w_p. The initial $\bar{n}$ is much lower with added diluent. The cause of this is most logically that which is central to our mechanistic hypotheses: the average termination rate coefficient $\langle k_t \rangle$ is increased by addition of diluent, because mobile short chains propagate to longer ones more slowly and are thus more likely to terminate. This interpretation suggests that the data with added diluent should have a different population distribution of growing chains compared to that of an undiluted system at the same w_p. Therefore, the diluent data should provide a meaningful test of the model. Referring to Figure 3, it is apparent that the large effect

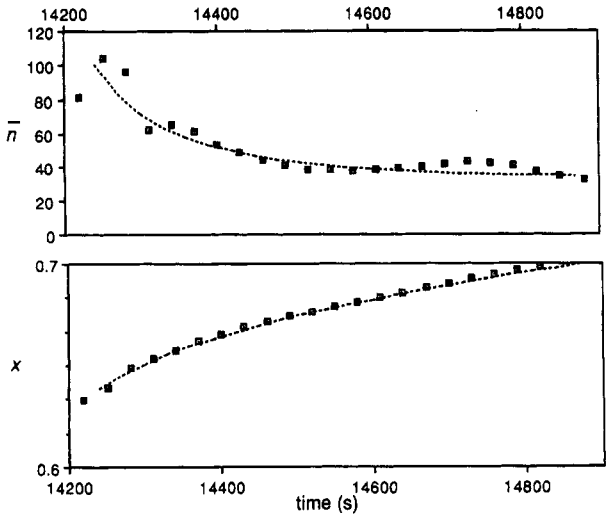

Figure 4. Fraction conversion x and $\bar{n}$ as functions of time after removal from the radiation source (relaxation data) without diluent. Time measured from start of run; removal from source occurred at 14 200 s. Initial $w_p = 0.82$. Points: experiment. Lines: simulation with same parameters as give optimal accord with data of Figure 2.

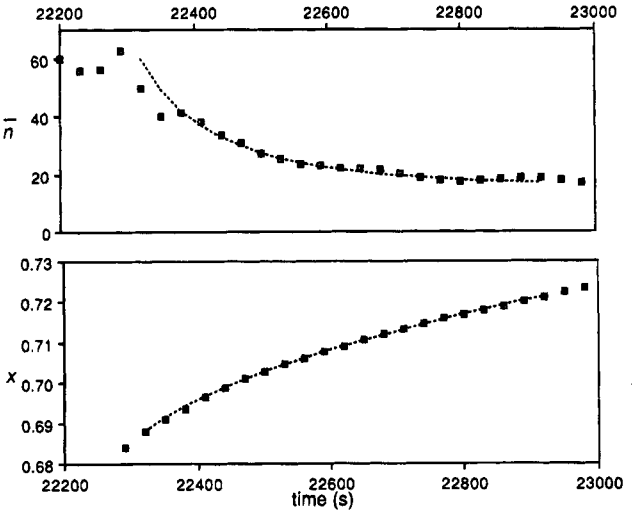

Figure 5. Fraction conversion x and $\bar{n}$ as functions of time after removal from the radiation source (relaxation data) with 15 mol % benzene diluent. Time measured from start of run; removal from source occurred at 22 250 s. Initial $w_p = 0.78$. Points: experiment. Lines: simulation with best fit parameters of Figure 2.

introduced by dilution is predicted extremely well *by the same parameters as fit the undiluted data*. Considering the sensitivity of the model to certain parameters, the fact that no parameters have been adjusted at all here is seen as an achievement and suggests overall correctness of the model assumptions.

Predictions of Kinetics at Different w_p. We now test the model against data obtained at high w_p. Figures 4 and 5 show the results of experiments and simulations of relaxation kinetics for the nondiluted system at $w_p = 0.82$ (cf. 0.71 for Figures 2 and 3) and the diluted system at $w_p = 0.78$. The parameters used to obtain the calculated dependence were exactly the same as those chosen and calibrated for the lower w_p relaxation. The results show excellent agreement with the experimental data, even though the overall relaxation rate changes drastically. Figure 6 displays the same information for a relaxation starting at $w_p = 0.55$ for an undiluted experiment. Comparison of conversion

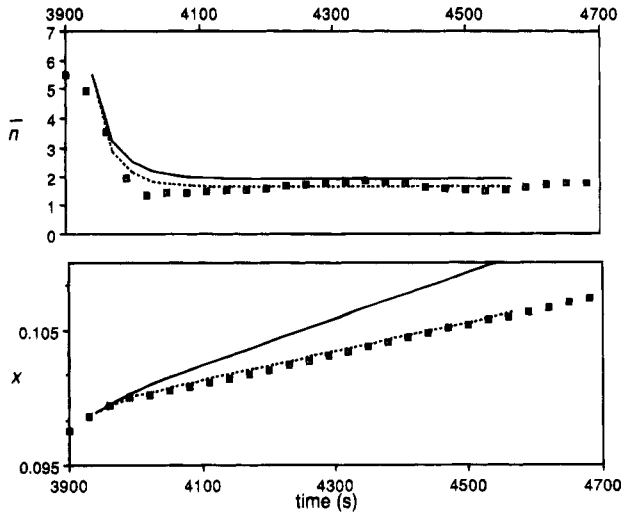

Figure 6. Fraction conversion x and $\bar{n}$ as functions of time after removal from the radiation source (relaxation data) without diluent. Time measured from start of run; removal from source occurred at 3900 s. Initial $w_p = 0.55$. Points: experiment. Lines: (—) simulation with benchmark parameters from Figure 2; (• • •) simulation as before, but with $p = 1.2$.

as a function of time appears to indicate that the accord between model and experiment, using the same parameters as for higher conversion, is poor. However, if the comparison instead is made with $\bar{n}$ (which is equivalent to rate), the actual diversion of the model from experiment is not great. As shown in Figure 6, agreement between theory and experiment can be brought about by increasing p from 0.35 to 1.2 (while, importantly, retaining the same $\varrho_{thermal}$); the same parameters also reproduce data with diluent. While in fact one would expect p to *decrease* with lower w_p, as discussed earlier, this parameter change is equivalent to assuming (as is more reasonable) that p remains constant but, for example, that the value of D_{mon} is somewhat higher at the lower w_p than measured for penetrants as shown in the data in Figure 1. It is apparent that accord could be attained by any one of several minor parameter adjustments, as discussed above. We do not carry out this curve-fitting exercise here but instead note that the semiquantitative accord seen in Figure 6 with the "raw" parameters suggests that the modeling encompasses the correct physical processes.

Data with Chemical Initiator. The next test is of the model's ability to predict the overall rate behavior with chemical initiator over a wide range of w_p. Unlike γ-relaxation data, data obtained with chemical initiator are sensitive to radical creation events (i.e., entry) as well as termination. For this reason, it is unwise to use chemically initiated data *alone* to learn about termination processes. However, once knowledge about termination has been gained *independently* using γ-relaxation, chemically initiated rate data over the same range of conversion can be used to learn about entry. In particular, our data enable us to test the aqueous-phase control model for entry[26,36] which leads to eq 24. In carrying out a simulation, account must be taken, in using eq 1 for the termination of species arising from initiator, that an i-mer contains i monomer units plus a sulfate end group. Also, due to uncertainty in the variation of $k_{p,aq}^{i}$ with i, it is not certain whether 2 or 3 monomer units must add to a sulfate radical before entry can occur.[26] For these reasons, separate simulations were carried out using both $z = 2$ and 3 for

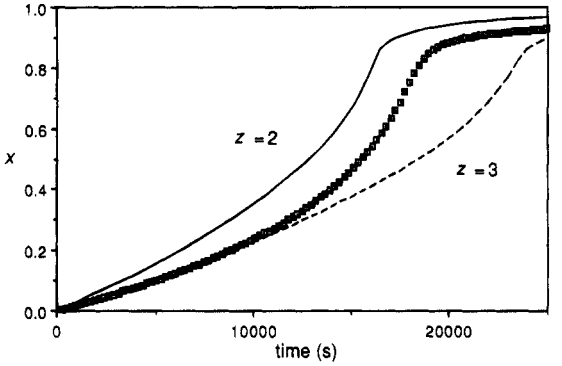

Figure 7. Fraction conversion x as a function of time for chemically initiated system; initiator = 1.1×10^{-3} mol dm^{-3} persulfate. Points: experiment. Lines: simulations with different values of z, the chain length of the entering species.

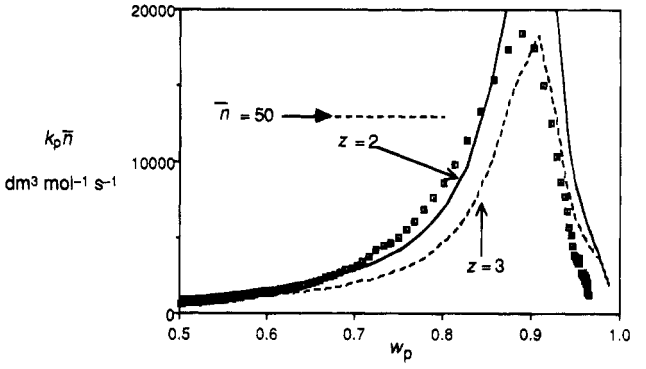

Figure 8. Data from simulations of Figure 7 here presented as $k_p\bar{n}$ as a function of conversion. Points: experiment. Lines: simulations. Values of $\bar{n}$ beyond where k_p becomes diffusion-controlled ($w_p \approx 0.85$) cannot be inferred from these experimental data, since $k_p(w_p)$ is not known; since k_p is constant at lower w_p, $\bar{n}$ values for $w_p \lesssim 0.85$ can be inferred from the data, and a reference value of $\bar{n} = 50$ is indicated for this purpose.

Table 3. Components of Total Entry Rate Coefficient (s^{-1}) Used for Simulations of Figures 7 and 8 (Shown for the Initial w_p)

z	$\varrho_{initiator}$	$\varrho_{thermal}$
2	0.081	0.027
3	0.017	0.027

initiator-derived radicals. The effect this has on $\varrho_{initiator}$ is shown in Table 3, which compares ϱ values used in simulations.

The results of simulations are displayed in Figures 7 and 8. The chemically initiated data cover a large range in conversion: from $w_p = 0.50$ up to 0.96. In comparing experimental and calculated rate results, we have used the product $k_p\bar{n}$, since k_p may well become diffusion controlled at higher w_p; hence, a unique value of $\bar{n}$ cannot be obtained from the observed polymerization rate at high w_p, since there are at present no experimental data on $k_p(w_p)$ for styrene (such data can in principle be obtained using EPR,[65-71] in which case the rate data in the present paper could then be reprocessed to yield the additional information of $\bar{n}$ up to $w_p = 0.96$). However, it will be seen that even without this additional information the present data remain informative.

The data are presented in Figures 7 and 8 in two different ways: conversion as a function of time (Figure 7) and $k_p\bar{n}$ as a function of w_p (Figure 8). The latter is a better means of testing the model assumptions in systems such as the present where there is a large range of w_p, for reasons discussed earlier: a relatively small mismatch in $\bar{n}$ in the gel regime (when $\bar{n}$ is rapidly changing) can result in a large difference in conversion at a later time. For reference, Figure 8 shows the value of $k_p\bar{n}$ where $\bar{n} = 50$ in the event of k_p being chemically controlled ($k_p = 2.6 \times 10^2$ dm^3 mol^{-1} s^{-1}); this experimental $\bar{n}$ can be firmly identified, since it occurs in a conversion regime significantly below where k_p is expected to become diffusion-controlled.

Figure 8 shows that the predictions of the model, *which now includes a model for entry*, are in quite acceptable agreement with experiment. In claiming this, several mitigating circumstances need to be borne in mind: (i) If comparison is made only with conversion as a function of time, accord seems poor (Figure 7), but that is largely a consequence of relatively small mismatches in $\bar{n}$, as explained above. (ii) A limitation of the simulations is that conversion-independent k_p has been used. Thus k_p is overestimated at high w_p, which of itself results in both x and $k_p\bar{n}$ being overestimated at high conversions, and also affects $\bar{n}$ through the role of k_p in determining the R_i. (iii) We have used here the w_p-independent value of $p = 0.35$, but our relaxation simulations suggested that this *modeling* parameter has a higher value at $w_p \approx 0.5$. Indeed, with $z = 2$ our simulated $\bar{n}$ are too high at early w_p (see Figures 7 and 8)—using a higher p would lower these $\bar{n}$.

6. Mechanistic Inferences

The accord between predictions of the overall kinetics and the data, when these data are highly sensitive to termination kinetics, suggests an overall correctness to our physical picture. The simulations can then be used to make a number of mechanistic inferences.

Entry. The first inference is that the data of Figure 8 are in accord with the model for entry of eqs 19–23. Although the entry rate coefficient (or initiator efficiency) cannot be measured without modeling in this high-$\bar{n}$ system (unlike low-$\bar{n}$, or "zero-one" systems, when ϱ can be inferred from appropriate conversion/time data in an essentially model-free fashion[26]), the simulations of Figures 7 and 8 imply the correctness of the entry model. It is important in this regard to note that the concentration of styrene in the aqueous phase varies strongly over the course of the data shown in Figures 7 and 8, and eq 24 predicts that a large variation in C_W would lead to a large change in initiator efficiency in systems such as styrene, in which aqueous-phase termination is a major kinetic process. Indeed, calculations with the data of Table 2 (see section 3) suggest that the initiator efficiency decreases from 27% without diluent to 9% with the addition of 15% benzene.

A complication with this inference is that there is a very fast reaction of benzene with $SO_4^{\bullet-}$.[72] The observed rate coefficient is 3×10^9 dm^3 mol^{-1} s^{-1}, a value that is about the same as k_{pi} for reaction of $SO_4^{\bullet-}$ with styrene. The observation that there is an overall reduction in initiator efficiency upon addition of benzene suggests that the species formed from reaction of benzene with $SO_4^{\bullet-}$ is inert. Quantification of this effect on the entry process requires more accurate values for these two rate coefficients than are presently available.

Rate at High Conversion. It is seen in Figure 8 that both experimental and simulated values of $k_p\bar{n}$ show a decrease at high w_p. Recall that the *simulations* assumed a *constant* k_p, although it is likely that in actuality this quantity would decrease with w_p for (say) $w_p \gtrsim 0.85$. The decrease in $k_p\bar{n}$ seen in the simulations

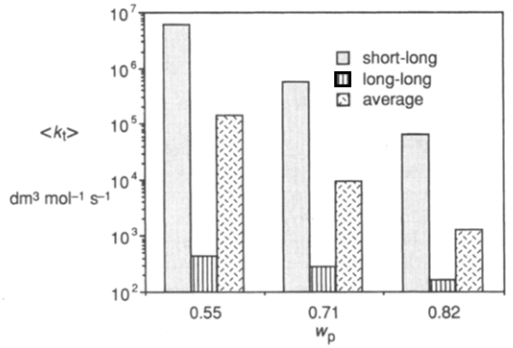

Figure 9. Calculated average termination rate coefficient, $\langle k_t \rangle$, and the components from short-long and long-long events, for different w_p. These calculated values are for the conditions of Figures 8 and 7, with $z = 2$.

obviously therefore arises because the simulated value of $\bar{n}$ decreases at high w_p. The reason for this is as follows. At very high conversion, the monomer concentration is low, and hence it takes more time for short chains to become long chains by propagation. (This effect will actually be enhanced if k_p is decreasing due to being diffusion controlled.) Since short chains have the highest rate coefficient for termination, this can mean that the overall termination rate can increase at high w_p *provided* that the increased relative number of short chains is not offset by the decrease in their diffusion coefficient that also occurs with increasing w_p (Figure 1). This indeed is obviously the case for the parameters chosen for the simulations.

The *observed* decrease in $k_p\bar{n}$ in Figure 8 can therefore be ascribed to one or both of two causes: the increase in the relative numbers of short chains just discussed and/or a decrease in k_p at high w_p. The data presently available are insufficient to establish the relative importance of these two possibilities, especially because the accord between the present simulations (with a constant k_p) and experimental data is only semiquantitative at the highest w_p.

Dominant Events in Termination. A number of inferences can be made about termination kinetics. Figure 9 shows, for different w_p, the calculated average termination rate coefficient from eq 18, and its two components from long−long and short−long termination events. We define the short−long component as

$$\langle k_t \rangle \text{ (short−long)} = \frac{\sum_{i=1}^{Z}\sum_{i=Z+1}^{\infty} k_t^{ij} R_i R_j}{\sum_{i=1}^{Z} R_i \sum_{j=Z+1}^{\infty} R_j} = \frac{\sum_{i=1}^{Z} k_t^{iL} R^i}{\sum_{i=1}^{Z} R_i} \qquad (30)$$

where, as a reminder, $Z = 180$ has been used. The average value $\langle k_t \rangle$ is a weighted sum of these short−long and long−long components, the weighting being the relative populations of long and short chains. This information can be used to understand the nature of the gel effect, as follows. It is apparent from Figure 9 that, as w_p increases, the average k_t decreases, as expected. One sees that the major contribution is always from termination between a long and a short chain. However, it is apparent that the proportion of short−long events diminishes as w_p increases. The decrease in *average* k_t which gives rise to the gel effect must arise from the decrease in the short−long termination rate. Now, the gel effect is a phenomenon that is to be properly understood in terms of a whole spectrum of D_i^{com} values. It is emphasized that there is no single one of these transitions to which one can generally ascribe the origin of the gel effect in all systems. However, modeling suggests that the decrease in average k_t which gives rise to the gel effect is usually due to the following effects.

(1) There are the effects that decrease short−long values of k_t^{ij}: (a) As w_p increases, viscosity increases, and so D_{mon}, and indeed all D_i^{com}, decrease. (b) As w_p increases, short-chain diffusion becomes a stronger function of chain length. This is reflected in chains becoming entangled at shorter chain lengths (i.e., X_c decreasing with increasing w_p—see eq 29—in the present model) and the short-chain-diffusion scaling exponent u increasing with w_p (eq 27).

(2) Coupled to the above effects is that of lower short−long k_t^{ij} resulting in a greater proportion of chains growing to be longer, and thus less mobile. This suggests that the gel effect also has its origin in a tilt in the population of radicals toward longer chain lengths, this lowering the overall $\langle k_t \rangle$.

Given the above, it is evident that there are two senses in which it might be said that the gel effect is "autocatalytic" or "autoaccelerating": (i) driving a system to higher conversions results in higher w_p, and so in lower $\langle k_t \rangle$ and even faster rates; and as well as this traditional meaning (ii) there is the more subtle effect of the lower k_t^{ij} resulting in an R_i distribution that is more weighted toward higher i, which also causes a lower $\langle k_t \rangle$, and so higher rates.

Thermal Entry. Information about the thermal entry rate coefficient can also be inferred from the data. A value of $\varrho_{thermal}$ can be inferred from the data fitting, with and without added benzene diluent. This fitting shows no significant difference in the value of $\varrho_{thermal}$ when benzene is added. The experimental results for monomer partitioning between particles and the aqueous phase show that the aqueous phase concentration of styrene with 15% dilution by benzene is approximately half the undiluted value. If thermal entry were, as is believed to be the case for chemical initiation, influenced by aqueous-phase growth, the rate at 15% dilution should therefore be substantially decreased. Because $\varrho_{thermal}$ is found to be unchanged by addition of diluent, thermal entry cannot be controlled by aqueous-phase propagation, a conclusion which is consistent with the effects on $\varrho_{thermal}$ of adding an aqueous-phase spin trap.[73] These results are consistent with thermal entry in styrene originating either on or within the particle. Moreover, they suggest that, whatever is the origin of thermal entry, there is no rate-determining step involving particle-phase monomer.

7. Conclusions

The overall objective of these experimental studies was to test a description of termination in which the rate coefficient for termination is obtained from the Smoluchowski equation and which depends explicitly on the degrees of polymerization of the two terminating chains. The data comprised the rates of relaxation of a seeded styrene emulsion polymerization after removal from the source of initiating radicals (a γ-radiolysis source). Data were obtained over a range of polymer weight fraction and with and without the addition of an inert diluent. These conditions are expected to give rise to different distributions of the lengths of propagating chains and therefore provide a stringent test of the

assumed model. Indeed, the observed relaxation (and in-source) behavior was seen to vary strongly with these changed experimental conditions. The model for k_t^{ij} is a "molecular-level" one, and the only parameter therein whose value is not known with moderate precision is the probability of spin flip of two radicals in a solvent cage, as a function of their degrees of polymerization and of w_p. Even then, this factor is expected to be close to $^1/_4$ for interactions involving at least one short chain. Treating this quantity as an adjustable parameter, it was evaluated as 0.35 by fitting to a single set of relaxation data (at $w_p = 0.71$, without added diluent). The resulting parametrization was found to provide a good fit to data with added diluent, for different values of w_p (over the range 0.5–0.82) and moreover to fit data from a quite different system where initiation was by persulfate, rather than γ-radiolysis. This strongly suggests the qualitative and quantitative correctness of the model.

The simulations were then used to draw a number of further inferences. It has been found that termination kinetics are dominated by encounters between short chains (formed both by entry and by transfer) and long, entangled ones. The origin of the gel effect (which, as seen in Figure 8, has been rather successfully modeled) is that the short–long termination rate coefficient decreases with w_p, which is a consequence both of short-chain diffusion rates decreasing and the radical distribution becoming longer.

The rate coefficients for entry with chemical initiator that are consistent with the data lend support to a model for this process. This model assumes that (for a monodisperse particle size distribution) entry occurs if and only if a radical attains a sufficient degree of polymerization to become surface-active; the rate-determining events for entry are thus propagation and termination in the aqueous phase. Our data also support earlier conclusions that background thermal entry does not involve aqueous-phase events.

Acknowledgment. We gratefully acknowledge the support of the Australian Institute of Nuclear Science and Engineering, the Emulsion Polymerization Foundation (SEP) of Eindhoven University of Technology, The Netherlands Organization for Scientific Research (NWO), the Australian Research Council, and provision of resources by the University of Sydney Electron Microscope Unit.

References and Notes

(1) Trommsdorff, E.; Kohle, E.; Lagally, P. *Makromol. Chem.* **1948**, *1*, 169.
(2) Norrish, R. G. W.; Smith, R. R. *Nature* **1942**, *150*, 336.
(3) Clay, P. A.; Gilbert, R. G. *Macromolecules* **1995**, *28*, 552.
(4) Yamada, B.; Yoshikawa, E.; Miura, H.; Otsu, K. *Makromol. Chem., Rapid Commun.* **1992**, *13*, 531.
(5) Bowry, V. W.; Ingold, K. U. *J. Am. Chem. Soc.* **1992**, *114*, 4992.
(6) Benson, S. W.; North, A. M. *J. Am. Chem. Soc.* **1962**, *84*, 935.
(7) Gilbert, R. G.; Smith, S. C. *Theory of Unimolecular and Recombination Reactions*; Blackwell Scientific: Oxford and Cambridge, MA, 1990.
(8) Cardenas, J.; O'Driscoll, K. F. *J. Polym. Sci., Polym. Chem. Ed.* **1976**, *14*, 883.
(9) Cardenas, J.; O'Driscoll, K. F. *J. Polym. Sci., Polym. Chem. Ed.* **1977**, *15*, 1883.
(10) Tulig, T. J.; Tirrell, M. *Macromolecules* **1981**, *14*, 1501.
(11) Soh, S. K.; Sundberg, D. C. *J. Polym. Sci., Polym. Chem. Ed.* **1982**, *20*, 1299.
(12) Olaj, O. F.; Zifferer, G.; Gleixner, G. *Macromolecules* **1987**, *20*, 839.
(13) Bamford, C. H. *Eur. Polym. J.* **1989**, *25*, 683.
(14) Mahabadi, H. K. *Macromolecules* **1985**, *18*, 1319.
(15) Mahabadi, H. K. *Macromolecules* **1991**, *24*, 606.
(16) Russell, G. T.; Gilbert, R. G.; Napper, D. H. *Macromolecules* **1992**, *25*, 2459.
(17) Russell, G. T.; Gilbert, R. G.; Napper, D. H. *Macromolecules* **1993**, *26*, 3538.
(18) Ley, G. J. M.; Schneider, C.; Hummel, D. O. *J. Polym. Sci., C* **1969**, *27*, 119.
(19) Lansdowne, S. W.; Gilbert, R. G.; Napper, D. H.; Sangster, D. F. *J. Chem. Soc., Faraday Trans. 1* **1980**, *76*, 1344.
(20) Adams, M. E.; Russell, G. T.; Casey, B. S.; Gilbert, R. G.; Napper, D. H.; Sangster, D. F. *Macromolecules* **1990**, *23*, 4624.
(21) Ballard, M. J.; Napper, D. H.; Gilbert, R. G.; Sangster, D. F. *J. Polym. Sci., Polym. Chem. Ed.* **1986**, *24*, 1027.
(22) Ballard, M. J.; Napper, D. H.; Gilbert, R. G. *J. Polym. Sci., Polym. Chem. Ed.* **1984**, *22*, 3225.
(23) Ugelstad, J.; Hansen, F. K. *Rubber Chem. Technol.* **1976**, *49*, 536.
(24) Nomura, M.; Harada, M.; Nakagawara, K.; Eguchi, W.; Nagata, S. *J. Chem. Eng. Jpn.* **1970**, *4*, 160.
(25) Nomura, M. In *Emulsion Polymerization*; Piirma, I., Ed.; Academic: New York, 1982; p 191.
(26) Casey, B. S.; Morrison, B. R.; Gilbert, R. G. *Prog. Polym. Sci.* **1993**, *18*, 1041.
(27) Morrison, B. R.; Casey, B. S.; Lacík, I.; Leslie, G. L.; Sangster, D. F.; Gilbert, R. G.; Napper, D. H. *J. Polym. Sci., Part A: Polym. Chem.* **1994**, *32*, 631.
(28) Lichti, G.; Sangster, D. F.; Whang, B. C. Y.; Napper, D. H.; Gilbert, R. G. *J. Chem. Soc., Faraday Trans. 1* **1984**, *80*, 2911.
(29) *Polymer Handbook*, 3rd ed.; Brandrup, A., Immergut, E. H., Eds.; Wiley-Interscience: New York, 1989.
(30) Morrison, B. R.; Piton, M. C.; Winnik, M. A.; Gilbert, R. G.; Napper, D. H. *Macromolecules* **1993**, *26*, 4368.
(31) Russell, G. T. *Macromol. Theory Simul.*, in press.
(32) Schulz, G. V. *Z. Phys. Chem. (Frankfurt am Main)* **1956**, *8*, 290.
(33) Russell, G. T.; Napper, D. H.; Gilbert, R. G. *Macromolecules* **1988**, *21*, 2133.
(34) Fischer, H.; Henning, P. *Acc. Chem. Res.* **1987**, *20*, 200.
(35) Tarasov, V. F.; Ghatlia, N. D.; Avdievich, N. I.; Shkrob, I. A.; Buchachenko, A. L.; Turro, N. J. *J. Am. Chem. Soc.* **1994**, *116*, 2281.
(36) Maxwell, I. A.; Morrison, B. R.; Napper, D. H.; Gilbert, R. G. *Macromolecules* **1991**, *24*, 1629.
(37) Hawkett, B. S.; Napper, D. H.; Gilbert, R. G. *J. Chem. Soc., Faraday Trans. 1* **1980**, *76*, 1323.
(38) Kast, H.; Funke, W. *Makromol. Chem.* **1981**, *182*, 1553.
(39) Said, Z. F. M.; Hassan, S. A.; Dunn, A. S. In *Emulsion Polymers and Emulsion Polymerization*; Bassett, D. R., Hamielec, A. C., Eds.; ACS Symposium Series 165; American Chemical Society: Washington, DC, 1981; p 471.
(40) Mills, M. F.; Gilbert, R. G.; Napper, D. H. *Macromolecules* **1990**, *23*, 4247.
(41) Mills, M. F.; Gilbert, R. G.; Napper, D. H.; Croxton, C. A. *Macromolecules* **1993**, *26*, 3563.
(42) Mills, M. F.; Gilbert, R. G.; Napper, D. H.; Rennie, A. R.; Ottewill, R. H. *Macromolecules* **1993**, *26*, 3553.
(43) Russell, G. T. *Macromol. Theory Simul.* **1994**, *3*, 439.
(44) Lane, W. H. *Ind. Eng. Chem.* **1946**, *18*, 295.
(45) Mahabadi, H. K.; O'Driscoll, K. F. *J. Macromol. Sci. Part, A: Chem.* **1977**, *11*, 967.
(46) Buback, M.; Garcia-Ribio, L. H.; Gilbert, R. G.; Napper, D. H.; Guillot, J.; Hamielec, A. E.; Hill, D.; O'Driscoll, K. F.; Olaj, O. F.; Shen, J.; Solomon, D.; Moad, G.; Stickler, M.; Tirrell, M.; Winnik, M. A. *J. Polym. Sci., Polym. Lett. Ed.* **1988**, *26*, 293.
(47) Hutchinson, R. A.; Aronson, M. T.; Richards, J. R. *Macromolecules* **1993**, *26*, 6410.
(48) Dainton, F. S.; James, D. G. L. *J. Polym. Sci.* **1959**, *39*, 299.
(49) Dainton, F. G.; Eaton, R. S. *J. Polym. Sci.* **1959**, *39*, 313.
(50) Sangster, D. F.; Davison, A. *J. Polym. Sci., Polym. Symp.* **1975**, *49*, 191.
(51) Behrman, E. J.; Edwards, J. O. *Rev. Inorg. Chem.* **1980**, *2*, 179.
(52) Sarkar, S.; Adhikari, M. S.; Benerjee, M.; Konar, R. S. *J. Appl. Polym. Sci.* **1988**, *35*, 1441.
(53) Maxwell, I. A.; Kurja, J.; van Doremaele, G. H. J.; German, A. L.; Morrison, B. R. *Makromol. Chem.* **1992**, *193*, 2049.
(54) Heuts, J. P. A.; Radom, L.; Gilbert, R. G., manuscript in preparation.
(55) Casey, B. S.; Mills, M. F.; Sangster, D. F.; Gilbert, R. G.; Napper, D. H. *Macromolecules* **1992**, *25*, 7063.
(56) Ferry, J. D. *Viscoelastic Properties of Polymers*, 2nd ed.; Wiley-Interscience: New York, 1980.

(57) Pickup, S.; Blum, F. D. *Macromolecules* **1989**, *22*, 3961.
(58) Kosfeld, R.; Goffloo, K. *Kolloid Z. Z. Polym.* **1971**, *247*, 801.
(59) Goffloo, K.; Kosfeld, R. *Angew. Makromol. Chem.* **1974**, *37*, 105.
(60) Landry, M. R.; Gu, Q. *Macromolecules* **1988**, *21*, 1158.
(61) Faldi, A.; Tirrell, M.; Lodge, T. P.; von Meerwall, E. D. *Polym. Prepr. (Am. Chem. Soc., Div. Polym. Chem.)* **1991**, *32*, 400.
(62) Lee, J. A.; Frick, T. S.; Huang, W. J.; Lodge, T. P.; Tirrell, M. *Polym. Prepr. (Am. Chem. Soc., Div. Polym. Chem.)* **1987**, *28*, 369.
(63) Heuts, J. P. A.; Clay, P. A.; Christie, D. I.; Piton, M. C.; Hutovic, J.; Kable, S. H.; Gilbert, R. G. *Prog. Pac. Polym. Sci., Proc.* **1994**, *3*, 203.
(64) Piton, M. C.; Gilbert, R. G.; Chapman, B. E.; Kuchel, P. W. *Macromolecules* **1993**, *26*, 4472.
(65) Ballard, M. J.; Gilbert, R. G.; Napper, D. H.; Pomery, P. J.; O'Sullivan, P. W.; O'Donnell, J. H. *Macromolecules* **1986**, *19*, 1303.
(66) Tonge, M.; Pace, R.; Gilbert, R. G. *Macromol. Chem. Phys.* **1994**, *195*, 3159.
(67) Lau, W.; Westmoreland, D. G.; Novak, R. W. *Macromolecules* **1987**, *20*, 457.
(68) Yamada, B.; Kageoka, M.; Otsu, T. *Polym. Bull.* **1992**, *28*, 75.
(69) Yamada, B.; Kageoga, M.; Otsu, T. *Macromolecules* **1991**, *24*, 5234.
(70) Yamada, B.; Kageoka, M.; Otsu, T. *Macromolecules* **1992**, *25*, 4828.
(71) Yamada, B.; Kageoka, M.; Otsu, T. *Polym. Bull.* **1992**, *29*, 385.
(72) Neta, P.; Madhavan, V.; Zemel, H.; Fessenden, R. W. *J. Am. Chem. Soc.* **1977**, *99*, 163.
(73) Lacík, I.; Casey, B. S.; Sangster, D. F.; Gilbert, R. G.; Napper, D. H. *Macromolecules* **1992**, *25*, 4065.

MA946066U